available at www.sciencedirect.com
ScienceDirect
journal homepage: www.elsevier.com/locate/agrformet

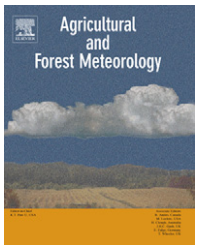

Evapotranspiration and regional probabilities of soil moisture stress in rainfed crops, southern India

Trent W. Biggs [a,*], *Prasanta K. Mishra* [b], *Hugh Turral* [c]

[a] *Department of Geography, San Diego State University, San Diego, CA 92182-4493, United States*
[b] *Central Soil &Water Conservation Research & Training Institute, Research Centre, Bellary, Karnataka 583104, India*
[c] *International Water Management Institute, Pelawatte, Battaramulla, Sri Lanka*

ARTICLE INFO

Article history:
Received 16 July 2007
Received in revised form
24 April 2008
Accepted 14 May 2008

Keywords:
Crop water use
Evapotranspiration
Soil moisture
Semi-arid tropics
India
Satellite methods
Regional

ABSTRACT

The long-term probability of soil moisture stress in rainfed crops was mapped at 0.5° resolution over the Krishna River basin in southern India (258,948 km^2). Measurements of actual evapotranspiration (E_a) from 90 lysimeter experiments at four locations in the basin were used to calibrate a non-linear regression model that predicted the combined crop coefficient (K_cK_s) as a function of the ratio of seasonal precipitation (P) to potential evapotranspiration (E_p). Crops included sorghum, pulses (mung bean, chickpea, soybean, pigeonpea) and oilseeds (safflower and sunflower). E_p was calculated with the Penman–Monteith equation using net radiation derived from two methods: (1) a surface radiation budget calculated from satellite imagery (E_pSRB) and (2) empirical equations that use data from meteorological stations (E_pGBE). The model of K_s as a function P/E_p was combined with a gridded time series of precipitation (0.5° resolution, 1901–2000) and maps of E_pSRB to define the probability distributions of P, P/E_p and K_s for sorghum at each 0.5° cell over the basin. Sorghum, a C4 crop, had higher E_a and K_s values than the C3 plants (oilseeds, pulses) when precipitation was low ($P < 1$ mm d^{-1}) but lower maximum E_a rates (3.3–4.5 mm d^{-1}) compared with C3 crops (oilseeds and pulses, 4.3–4.9 mm d^{-1}). The crop coefficient under adequate soil moisture (K_c) was higher than the FAO-56 crop coefficients by up to 56% for oilseeds and pulses. The seasonal soil moisture coefficient (K_s) for sorghum ranged from 1.0 under high rainfall (July–October) to 0.45 in dry seasons (November–March), showing strong soil moisture controls on E_a. E_pSRB calculated at the lysimeter stations was 4–20% lower than E_pGBE, with the largest difference in the dry season. K_c derived from E_pSRB was only slightly (2–4%) higher than K_c derived from E_pSRB, because the maximum E_a occurred during the monsoon when the differences between E_pSRB and E_pGBE were small. Approximately 20% of the basin area was expected to experience mild or greater soil moisture stress ($K_s < 0.80$) during the monsoon cropping season 1 year in every 2 years, while 70% of the basin experienced mild or greater stress 1 year in 10. The maps of soil moisture stress provide the basis for estimating the probability of drought and the benefits of supplemental irrigation.

* *Corresponding author*. Tel.: +1 619 594 0902; fax: +1 619 594 4938.
E-mail addresses: tbiggs@mail.sdsu.edu (T.W. Biggs), pkmbellary@rediffmail.com (P.K. Mishra), h.turral@cgiar.org (H. Turral).
0168-1923/$ – see front matter
doi:10.1016/j.agrformet.2008.05.012

1. Introduction

Rainfed crops cover more than 80% of global cropped area and account for 60–70% of global crop production, but production is frequently limited by drought and soil moisture stress (Wood et al., 2000). Supplemental irrigation is often proposed to increase yields of rainfed crops, mitigate soil moisture stress during dry periods, and alleviate poverty (Brugere and Lingard, 2003; Fox and Rockström, 2003; Oweis et al., 1998; Pereira et al., 2002). Supplemental irrigation may not be needed every year, so it is a risk mitigation strategy and its benefits best approached in a probabilistic context (Fox et al., 2005). Increasing pressure on water resources at river basin scales also suggests that supplemental irrigation projects need to be evaluated in a basin context in order to assess their impact on surface and groundwater resources. In a river basin, planning for supplemental irrigation and anticipating the consequences of interannual variability in precipitation for soil moisture stress can be approached by mapping the probability distributions of soil moisture stress at each location in the basin. Questions related to probability-based management of rainfed crops at the basin scale include: What is the probability that a given location will experience soil moisture stress in a randomly selected year? What fraction of the cropped area in a river basin experiences mild to severe moisture stress most years? How does the risk of moisture stress vary by crop type? Understanding the spatial patterns in the probability of soil moisture stress is essential for anticipating and mitigating its effects on crop yields and farmer incomes at river basin scales.

Soil moisture stress is indicated when the rate of actual evapotranspiration (E_a) falls below the potential rate for a given crop. Methods to estimate E_a and soil moisture stress may be grouped into three categories: ground-based measurements, satellite methods, and mathematical models. Ground-based measurements include lysimeters and *in situ* meteorological techniques such as eddy covariance (Paco et al., 2006) and Bowen ratio determination (Drexler et al., 2004; Inman-Bamber and McGlinchey, 2003). Weighing lysimeters measure changes in soil moisture over a cropping season and are often used to calibrate and validate other methods of estimating E_a (Dehghani Sanij et al., 2004; Mohan and Arumugam, 1994; Tyagi et al., 2000a). While improper site conditions may result in unreliable measurements (Allen et al., 1991), lysimeters are the generally accepted reference method for measuring actual crop water use under field conditions. Lysimeter measurements have been reported for several crops in India, including irrigated wheat (Singandhupe and Sethi, 2005), corn (Tyagi et al., 2003), sorghum (Tyagi et al., 2000b), and sunflower (Tyagi et al., 2000a), but they have not been used to quantify the relationship between precipitation and E_a for rainfed crops in India.

Satellite imagery has been used for regional estimation of E_a, particularly in irrigated areas (Bastiaanssen et al., 2002; Garatuza-Payan and Watts, 2005; Loukas et al., 2005). While thermal bands or the normalized difference vegetation index (NDVI) are useful for estimating the spatial variation in E_a during cloud-free periods, their application for probabilistic analysis of soil moisture stress in rainfed crops is limited by several factors: (1) cloud cover often prevents the use of imagery during the rainy season, when most rainfed crops are cultivated; (2) crop type must be determined simultaneously, but this is difficult where cultivated plots are smaller than the image pixel (Biggs et al., 2006); and (3) estimates of E_a are limited to the period of available imagery. These factors limit the use of satellite methods for determining the long-term variability and probability distributions of soil moisture stress in rainfed crops.

Mathematical models of E_a represent the processes affecting evapotranspiration with considerable variation in the level of detail. While simple models often require calibration to local measurements and cannot be readily applied to different regions, complex models are data intensive and may have significant parameter uncertainty (Schulz and Beven, 2003). The relatively simple FAO-56 method is commonly used to estimate E_a from ground-based climate data (Allen et al., 1998). It uses the Penman–Monteith equation for potential evapotranspiration, includes the effect of crop type with a crop coefficient (K_c), and represents the effect of soil moisture stress with a soil moisture coefficient (K_s). Both K_c and K_s values differ by climate and soil type in ways that make calibration to local measurements necessary for robust estimation of E_a. For example, default K_c values underestimate E_a measured with lysimeters from a variety of crops in India, including irrigated wheat (Singandhupe and Sethi, 2005), corn (Tyagi et al., 2003) and sunflower (Tyagi et al., 2000a). The soil moisture coefficient (K_s) also varies with precipitation, crop type, soil type, and the duration of dry periods. More complex models that use daily precipitation to describe soil water movement and uptake by roots may be used to estimate E_a, but such models are data intensive and difficult to parameterize, often resulting in large prediction uncertainty (Franks et al., 1997; Schulz and Beven, 2003). In particular, detailed models require daily precipitation values and detailed soil characteristics, which are often not available over large regions. Where data on both rainfall and soil type are limited, simple models may provide more robust estimates of regional patterns than complex models that have high parameter uncertainty.

Simple models of soil moisture stress based on seasonal precipitation can leverage historical datasets, which is necessary for defining the long-term probability distribution of soil moisture stress. Historical (1901–2000) datasets of monthly precipitation with global coverage (Mitchell et al., 2004) are readily available and may be used to define the probability distribution of seasonal rainfall and soil moisture stress over large areas. Use of these monthly datasets requires the development of models of E_a and soil moisture stress that can be calibrated to monthly or seasonal precipitation. While soil moisture stress also depends on the daily sequence of storm size and the length of dry periods between storms (Rodriguez-Iturbe et al., 2001), reliable daily data are often not available for long time periods at the regional scale. Forecasts of rainfall by both empirical (Rajeevan et al., 2004) and dynamic (Kumar et al., 2005) methods are commonly seasonal, so corresponding forecasts of soil moisture stress must be based on seasonal rainfall values.

At regional scales, even simple models of moisture stress require estimates of potential evapotranspiration (E_p), which is a function of air temperature, vapor pressure, wind speed, and net radiation (R_n). While data on temperature, vapor pressure, and wind speed are commonly available from meteorological stations, ground-based measurements of R_n are often not available in many parts of the world. Empirical

Please cite this article in press as: Biggs, T.W. et al., Evapotranspiration and regional probabilities of soil moisture stress in rainfed crops, southern India, Agric. Forest Meteorol. (2008), doi:10.1016/j.agrformet.2008.05.012

equations that predict shortwave and longwave radiation from surface meteorological measurements have been widely used to estimate radiation where measurements are not available (Allen et al., 1998; Supit and van Kappel, 1998). The equations use constant coefficients that are calibrated to observed meteorological conditions at single points or stations. This is problematic over large regions where the coefficients and the atmospheric conditions that affect them, including the vertical distribution of water vapor, aerosols and cloud properties, may vary spatially. Ground-based measurements of longwave radiation are often not available, and coefficients must be taken from the literature and assumed to be representative of the study area.

Satellite methods estimate shortwave and longwave radiation without the need for locally adjusted calibration coefficients. Satellite imagery has recently been employed to estimate R_n globally (Gupta et al., 1999), and will likely be an increasingly important data source for basin-scale estimates of R_n and E_a (Stewart et al., 1999). However, E_p values may differ according to the method used to estimate or measure radiation, so crop coefficients (K_c) that are back-calculated from observed E_a may also differ by E_p method (Singandhupe and Sethi, 2005). Each K_c has a radiation and E_p method embedded in it, and a crop coefficient derived from one method may not be appropriate for calculating E_a using R_n and E_p calculated from a different method. Estimation of E_a and soil moisture stress at regional scales requires comparison of E_p and K_c values derived from satellite-based radiation measurements with E_p and K_c values derived from ground-based estimates of radiation.

The objectives of this study were to: (1) compile available measurements of actual evapotranspiration (E_a) from lysimeters for different rainfed crops in southern India, (2) calculate crop and soil moisture coefficients using both satellite-based and ground-based estimates of radiation and potential evapotranspiration (E_p), (3) develop a simplified model of actual evapotranspiration that uses seasonal precipitation as input, and (4) use the model, long-term precipitation records and regional maps of E_p to define the probability distributions of soil moisture stress at 0.5° resolution over the Krishna Basin in southern India.

2. Study area

The Krishna Basin covers an area of 258,948 km^2 in southern India (Fig. 1A, Biggs et al., 2007a). The climate is sub-humid to semi-arid, with a narrow humid zone in the Western Ghats. Rainfall averages 840 mm y^{-1}, and ranges from 500 to 900 mm y^{-1} on the central Deccan Plateau to more than 1000 mm in the Delta and more than 2500 mm in parts of the Western Ghats. Most (84%) of the precipitation falls during the monsoon from June to October. Potential evapotranspiration (E_p) computed using the Penman–Monteith equation and net radiation data from the Surface Radiation Budget (Fig. 1B, see Section 3.3) is lowest in the Western Ghats (1050–1200 mm y^{-1}), and highest in the central plateau (1700–1820 mm y^{-1}) with intermediate values in the Krishna Delta (1300–1400 mm y^{-1}).

The geology of the basin is dominantly Archaen granite and gneiss, with Deccan basalts in the northwest. Soil depth (Fig. 2) ranges from shallow (<0.5 m, 30% of basin area) to moderately

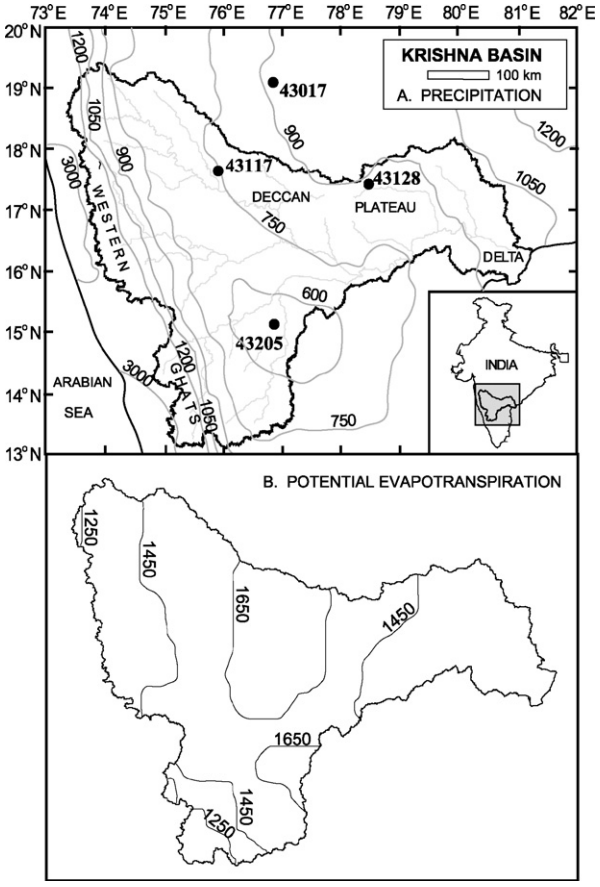

Fig. 1 – Location map of the Krishna Basin, southern India showing (A) annual precipitation (mm) and meteorological stations, and (B) annual potential evapotranspiration (mm) calculated using net radiation from satellite imagery (SRB). Numbers next to each station in (A) are the station codes from the Indian Meteorological Department.

deep (0.5–1 m, 26%) and deep (>1 m, 43%). Clay soils predominate (62% of basin area), followed by loam (16%), gravelly clay (13%) and gravelly loam (9%). The soils classify as Ustrorthents and Ustropepts, with limited Haplustalfs, Chromusterts, and Comborthids (Challa et al., 1996; Government of India, 1999; Sehgal et al., 1996). Soils are shallower in upslope positions and deeper (>0.9 m) downslope and along valley bottoms (Singh et al., 1999). One weathered profile on shallow soils in an upslope position of the granitic plateau consisted of 0.1–0.4 m of soil, 1–3 m of sandy regolith, 10–15 m of laminated saprolite, and fissured granite of 15–20 m (Dewandel et al., 2006). The regolith below the soil is often composed of sand or gravel (locally called *murrum*) that holds water and can provide moisture for crop growth (Singh et al., 1999). Crop roots extend into this layer, resulting in effective soils depths greater than 1 m, even where the soil is mapped as shallow. According to global maps (1:5,000,000), the soils in the Krishna Basin have an available water holding capacity (AWC) of 150–200 mm in the upper 1 m (Food and Agriculture Organization, 1995).

Rainfed crops grown in the basin include sorghum, lentils, millet, groundnut, and other oilseeds. Irrigated crops include rice, cotton, and chili in the eastern part of the basin, and sugarcane at the base of the Western Ghats (Biggs et al., 2006).

Please cite this article in press as: Biggs, T.W. et al., Evapotranspiration and regional probabilities of soil moisture stress in rainfed crops, southern India, Agric. Forest Meteorol. (2008), doi:10.1016/j.agrformet.2008.05.012

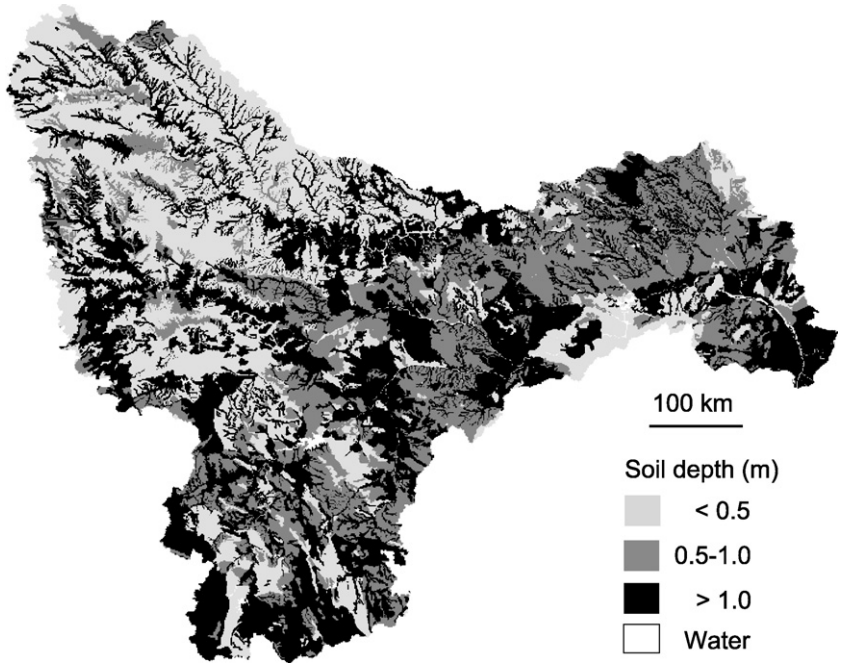

Fig. 2 – Soil depth in the Krishna Basin, digitized from 1:500,000 scale maps from Challa et al. (1996), Government of India (1999) and Sehgal et al. (1996).

One cropping season (*kharif*) coincides with the monsoon (June or July to October), and the second cropping season (*rabi*) occurs during the post-monsoon (October or November to March). With the exception of perennial crops, sugarcane, and some vegetable crops, most irrigated areas and all rainfed fields are left fallow in April and May.

3. Methods

3.1. *Lysimeter measurements*

Actual evapotranspiration (E_a) was measured with weighing lysimeters for seven different crops at four stations in and near the Krishna Basin by the Indian Meteorological Department (IMD) (Fig. 1, Tables 1 and 2). Crops included sorghum, pulses (mung bean, chickpea, soybean, pigeonpea), and oilseeds (sunflower, safflower). The lysimeters, manufactured by Avery Company India Ltd., were 1.3 m × 1.3 m by 0.9 m deep. The lysimeters were mounted so that the rim was level with the surrounding soil surface (Mohan and Arumugam, 1994). The average daily E_a, the number of measurements in each month, and the sowing and harvesting dates were available from the IMD. Crops received supplemental irrigation in four of the ninety experiments, and the depths of irrigation were available from the station managers. The soil was not wetted prior to sowing, so all E_a was derived from residual soil moisture at the time of sowing and from

Table 1 – Inventory of lysimeter data by crop for the four meteorological stations in the Krishna Basin

Crop	Varieties	Stations	N	Growing season (*d*)			Seasonal E_a (mm)		
				Min	Max	Med	Min	Max	Med
GRAINS									
Sorghum	CSH-1, CSH-6, CSH-9, M-35-1, Maldandi, SPV-86, R-16, CSV-15, R-19	43017, 43117, 43128, 43205	53	102	175	128	187	571	349
PULSES									
Gram	Vikas, Vijay, Vishal	43017, 43117	8	89	120	100	99	405	190
Chickpea	Annegiri, ICC-37	43128	7	97	120	100	116	177	153
Soybean	Macs-124, Monetta	43017	3	87	91	87	378	413	395
Pigeonpea	ICPL-84023	43128	1	123	123	123	433	433	433
OILSEEDS									
Safflower	Bhima, S-4, Manjira, A-1	43017, 43128, 43205	9	135	143	142	79	414	195
Sunflower	Modern, S-4, KBSH-1	43017, 43117, 43205	9	90	121	110	197	561	401

Med indicates the median.

Please cite this article in press as: Biggs, T.W. et al., Evapotranspiration and regional probabilities of soil moisture stress in rainfed crops, southern India, Agric. Forest Meteorol. (2008), doi:10.1016/j.agrformet.2008.05.012

Table 2 – Characteristics of the lysimeter stations

Station code	Location name	Soil texture	Rainfall (mm y^{-1})[a]	E_p (mm y^{-1})[b]	
				E_pGBE	E_pSRB
43017	Parbhani	Clay	946	1733	1536
43117	Solapur	Silty clay	779	1828	1612
43128	Hyderabad	Clay	819	1855	1549
43205	Bellary	Clay	522	1740	1624

E_pGBE is potential evapotranspiration (E_p) calculated with net radiation estimated from ground-based meteorological measurements, and E_pSRB is E_p calculated with net radiation from the surface radiation budget (SRB).
[a] Mean over 1951–1995.
[b] Mean for the period of available SRB data (1983–1995).

precipitation during the growing season. The timing of sowing varied from the beginning of the monsoon or *kharif* season (July) to the middle of the post-monsoon or *rabi* season (January). The texture of the soil used in the lysimeter experiments was clay or silty clay (Table 2).

All lysimeter stations were located on the semi-arid plateau, with a mean annual precipitation range of 522–946 mm (Table 2). Potential evapotranspiration (E_p) varied less than precipitation among the stations, with a range of 1536–1624 mm y^{-1}. See Section 3.3 for details of the E_p calculations.

3.2. Model of evapotranspiration and the crop coefficient

In the FAO-56 method (Allen et al., 1998), E_a is modeled as:

$$E_a = K_c K_s E_p \quad (1)$$

where K_c is the crop coefficient under adequate soil moisture (unitless), K_s is the soil moisture coefficient (0–1, unitless), and E_p is the potential evapotranspiration for a reference grass in mm d^{-1}. K_cK_s is the combined crop coefficient and includes the effect of both crop type and soil moisture stress. Soil moisture stress is indicated when K_s is less than 1.0 (Allen et al., 1998).

An exponential model of the relationship between seasonal P and E_a was developed:

$$E_a = E_d + E_w[1 - \exp(-\lambda_E P)] \quad (2)$$

where E_d is evapotranspiration under zero precipitation during the growing season (mm d^{-1}), E_w is the additional evapotranspiration under conditions of no soil moisture stress, λ_E is a parameter (mm^{-1}), and P is mean daily precipitation during the growing season (mm d^{-1}). For the few experiments where the crop received supplemental irrigation ($N = 4$), P includes the mean daily irrigation water applied during the growing season (mm d^{-1}). E_d was not zero due to residual soil moisture from the monsoon. While the amount of residual soil moisture at the beginning of the growing season may be important for controlling E_d, we did not find a correlation between E_a in the post-monsoon and rainfall in the preceding month or season. E_d is, therefore, treated as a constant and P is used as the predictor of seasonal evapotranspiration.

At regional scales, E_a also varies due to spatial variations in potential evapotranspiration (E_p). K_cK_s, the combined crop coefficient, can be calculated by dividing (2) by E_p, and the effect of E_p on soil moisture stress for a given precipitation depth may be accounted for by normalizing P by E_p:

$$K_cK_s = K_d + K_w\left[1 - \exp\left(-\frac{\lambda_K P}{E_p}\right)\right] \quad (3)$$

K_c is assumed to be constant over the region for a given crop, and is determined as the value of (3) at the maximum observed P/E_p. K_s for all lysimeter experiments is then calculated by dividing (3) by K_c. The parameters in Eqs. (2) and (3) are determined by fitting the model to observed data at the lysimeter stations using multidimensional, unconstrained nonlinear minimization of errors (Nelder–Mead) in MATLAB™ version 7.1.0.

Other models of E_a and K_s in the literature assume a linear relationship between soil moisture and K_s up to a threshold (Allen et al., 1998; Laio et al., 2001). The scatter in the data around the $E_a - P$ and $K_cK_s - P/E_p$ relationships in the Krishna Basin complicated the determination of a single threshold precipitation depth, while the exponential relationship does not require a threshold value. Additionally, the relationship between soil moisture and E_a may be linear, but the relationships in (2) and (3) are between P and E_a or P/E_p and K_cK_s, which may not be linear due to runoff and drainage. Finally, the main purpose of the model is not to propose a new relationship between P and E_a, but rather to use easily parameterized, empirical $E_a - P$ and $K_cK_s - P/E_p$ relationships to calculate the probability distributions of E_a and K_s based on a global precipitation dataset.

3.3. Potential evapotranspiration and net radiation

The Penman–Monteith equation (Allen et al., 1998) was used to calculate potential evapotranspiration (E_p) at each of the four lysimeter stations using the observed temperature, vapor pressure, wind speed, and two different methods of determining net radiation. In the first method, net radiation was calculated from empirical equations that use ground-based meteorological data (hereafter E_pGBE). The second method used satellite-based radiation values from NASA's surface radiation budget (hereafter E_pSRB). The two methods are described in detail in Sections 3.3.1 and 3.3.2.

Regional maps of monthly E_p were produced using the Penman–Monteith equation and the SRB data for radiation. Temperature, vapor pressure and wind speed were interpolated from 26 meteorological stations in the basin using linear relationships with elevation and distance inland, and

Please cite this article in press as: Biggs, T.W. et al., Evapotranspiration and regional probabilities of soil moisture stress in rainfed crops, southern India, Agric. Forest Meteorol. (2008), doi:10.1016/j.agrformet.2008.05.012

inverse-distance weighting of residuals (Biggs et al., 2007a; New et al., 1999).

3.3.1. Ground-based radiation

Measurements of shortwave radiation were available for two locations in the basin, and no measurements were available for longwave radiation. Where measurements of radiation are not available, ground-based meteorological measurements may be used as input to empirical equations that estimate shortwave and longwave radiation. For shortwave radiation, the Angstrom relation uses sunshine hours, the Hargreaves equation requires diurnal temperature range, and the modified Hargreaves equation uses diurnal temperature range and cloudiness (Supit and van Kappel, 1998). Data on sunshine hours were not available at all of the lysimeter stations, so the modified Hargreaves equation was used to estimate shortwave radiation (Biggs et al., 2007b). The Hargreaves coefficients were calibrated to measurements of shortwave radiation from two pyranometers in the basin (Biggs et al., 2007b). Net longwave radiation was estimated from the FAO-56 method (Allen et al., 1998), which requires ground-based measurements of temperature, vapor pressure, and shortwave radiation estimated with the modified Hargreaves equation.

3.3.2. Satellite-based radiation

Shortwave and longwave radiation data from the Surface Radiation Budget (SRB) version 2 were downloaded from the NASA Langley Research Center website (http://eosweb.larc.nasa.gov, accessed June 2007). A full description of the method is available at the NASA website, including details on the algorithms and satellite data utilized. In sum, the SRB algorithm for shortwave radiation uses satellite-based measurements of precipitable water, ozone, aerosols, and albedo to calculate atmospheric transmissivity and downwelling shortwave radiation at 1° spatial resolution. The SRB longwave algorithm uses a thermal infrared radiation transfer code and satellite measurements of precipitable water, cloud properties, and surface conditions (Fu et al., 1997; Stackhouse et al., 2001). Shortwave and longwave radiation were calculated at 3-hourly intervals and then aggregated to daily and monthly values. The long-term average shortwave and longwave radiation for each month were calculated for each 1° cell in the Krishna Basin for the years with available data (1983–1995).

The SRB has a mean bias of 6 W m^{-2} for down-welling shortwave and 1.7 W m^{-2} for longwave radiation, with root mean squared error (RMSE) of ±43 and ±13 W m^{-2} for shortwave and longwave, respectively. Comparison of the SRB shortwave data with pyranometer data in the central Krishna Basin gave a mean RMSE ranging from 9 to 23 W m^{-2} (Biggs et al., 2007b).

Albedo was set to 0.23 for both the GBE and SRB methods, as recommended by the FAO-56 (Allen et al., 1998). The SRB data could be used to calculate albedo, but those values would be at 1° spatial resolution and would include a heterogeneous mosaic of land cover types, including crops, rangelands, and bare soil. Future efforts to refine net radiation estimates could use spatially distributed albedo values or ground-based measurements of the shortwave radiation budget.

3.4. Cumulative probability distributions of precipitation and K_s

Grids of monthly precipitation with 0.5° resolution and continuous coverage from 1901 to 2000 were downloaded from the Climate Research Unit (CRU TS 2.1, http://www.cru.uea.ac.uk/cru/data/hrg.htm, accessed November 2007). The CRU grids were generated using quality-controlled data from meteorological stations (Mitchell and Jones, 2005) interpolated with a combination of thin-plate splines to generate global fields of climate normals (New et al., 1999), and exponential inverse-distance weighting to interpolate monthly anomalies (New et al., 2000). Total precipitation was calculated for the *kharif* (July–October) and *rabi* (October–January) seasons for each 0.5° cell in the Krishna Basin. The months defining these seasons correspond to the sowing and harvest dates reported for the lysimeter experiments on sorghum. The ratio of seasonal precipitation to seasonal E_p was calculated for each season and year using the E_pSRB maps.

The parameters of normal and gamma probability distributions were determined for the CRU precipitation data and P/E_p in each 0.5° cell using the method of moments. The $K_cK_s - P/E_p$ relationship (Eq. (3)) was then used to estimate K_s for each value of P/E_p. The predicted K_s values fit a beta distribution better than a normal or gamma distribution, so the parameters of the beta distribution were fit using the method of moments. Four locations in the basin were selected to illustrate the range of probability distributions of P, P/E_p, and K_s: the Krishna Delta, Western Ghats, the south-central plateau, and Hyderabad, the capital city of the State of Andhra Pradesh on the central plateau.

4. Results and discussion

4.1. Observed E_a and regression model coefficients

Seasonal E_a for all experiments ranged from 0.6 to 4.8 mm d^{-1} (Fig. 3). E_a and K_cK_s correlated positively with seasonal precipitation (P) or P/E_p (Fig. 4), which indicated strong soil moisture controls on E_a. The model of E_a (Eq. (2)) explained 71–95% of the variance in E_a (Table 3). The model of K_cK_s (Eq. (3)) explained less of the variance (49–90%) than the $E_a - P$ model. The $K_cK_s - P/E_p$ relationships for sorghum did not vary among the four lysimeter stations, so a single model was used for all sorghum data. A separate model was fit to the data for all oilseeds combined, and another model was fit to the data for all pulses combined.

The $E_a - P$ and $K_cK_s - P/E_p$ curves differed by the metabolic pathway of each crop. Sorghum, a C4 plant, had lower E_a and K_cK_s under adequate soil moisture than the C3 plants (oilseeds or pulses), but had higher E_a and K_cK_s under conditions of low precipitation than the C3 plants. This is expected based on C3 and C4 metabolism: C4 plants typically show lower evapotranspiration rates than C3 plants under conditions of adequate soil moisture (Hattendorf et al., 1988; Rachidi et al., 1993) but have higher E_a rates than C3 plants under conditions of soil moisture stress (Zhang and Kirkham, 1995). The lysimeter measurements in the Krishna Basin suggest that pulses also have high E_a rates, though pulses had lower E_a rates than

Please cite this article in press as: Biggs, T.W. et al., Evapotranspiration and regional probabilities of soil moisture stress in rainfed crops, southern India, Agric. Forest Meteorol. (2008), doi:10.1016/j.agrformet.2008.05.012

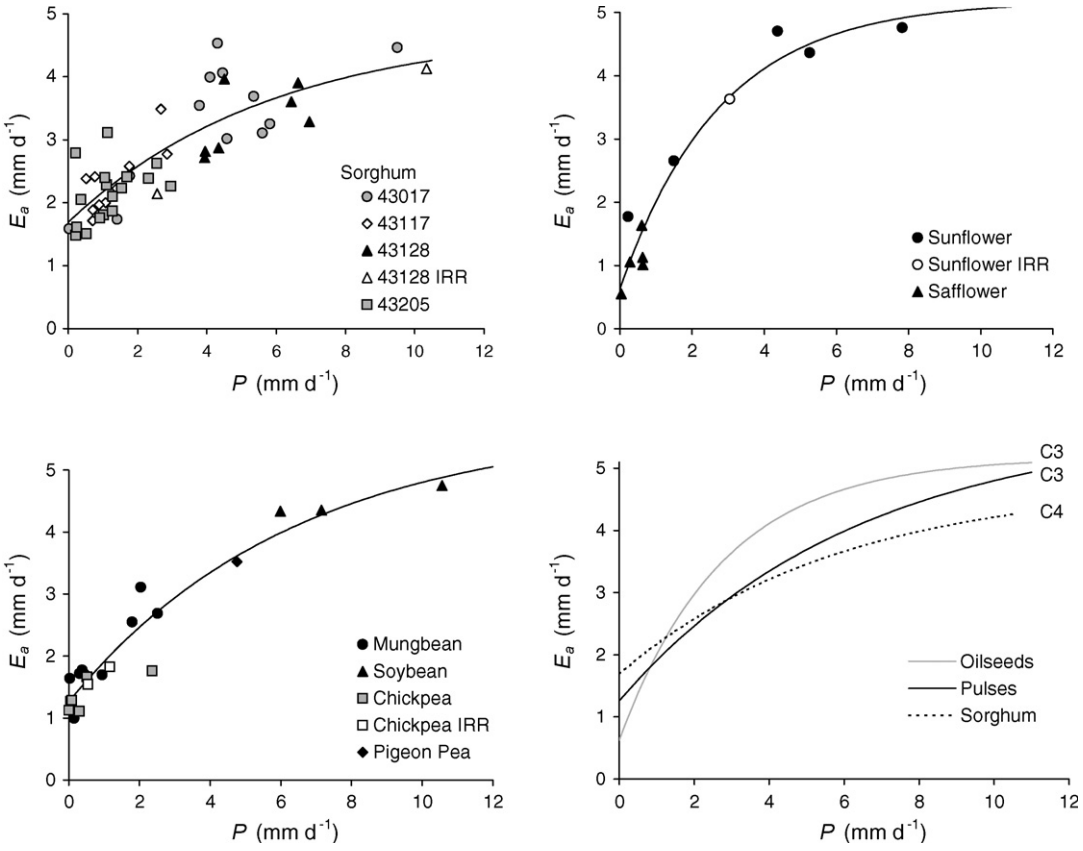

Fig. 3 – Precipitation versus evapotranspiration E_a observed in the lysimeter experiments by crop type. The lines indicate the model fits (Eq. (2)).

sunflower under moderate precipitation (1–8 mm d^{-1}). These K_c values differ from the K_c values from the FAO-56 method, which list higher K_c values for sorghum than for sunflower and pulses (Table 4). We conclude that the K_c and E_a values from oilseeds and pulses in the basin are consistently higher than sorghum, and E_a in the Krishna Basin (and probably other locations in India) should be modeled with these revised coefficients.

Crop coefficients under adequate soil moisture (K_c) were higher than the default FAO-56 values for oilseeds and pulses but not for sorghum (Table 4). The difference between the FAO-56 crop coefficients and coefficients derived from the lysimeters was larger after adjusting for the effect of non-standard conditions due to high relative humidity during the monsoon season. Other studies in India have shown similar results, where K_c values from C3 crops (sunflower, pulses) were higher than the FAO-56 values (Table 4).

Seasonal evapotranspiration (E_a) was greater than precipitation during the growing season for 31 of the 53 experiments on sorghum, particularly for experiments conducted during the post-monsoon season. When E_a is greater than P, the difference between P and E_a is the net change in soil moisture storage (ΔS). For the experiments with E_a greater than P, ΔS ranged from −10 to −329 mm, with a mean of −159 ± 88 mm. For comparison, the available soil water holding capacity (AWC) of a Vertic Inceptisol in the Krishna Basin ranged from 170–190 mm in the upper 125 cm of soil (Singh et al., 1999), and regional maps estimate AWC of 150–200 mm in the upper 1 meter (Food and Agriculture Organization, 1995). ΔS was between 0 and −200 mm for most (75%) of the lysimeter experiments where E_a was greater than P, suggesting that soil moisture storage was sufficient to supply E_a during most post-monsoon experiments, though at a rate significantly below the potential E_a of the crop. ΔS greater than 200 mm is possible given the likely range of AWC, but ΔS greater than 300 mm (N = 1 of 53) suggests measurement error or imperfect drainage from the lysimeter.

Table 3 – Regression parameters for the models of evapotranspiration (Eq. (2)) and the combined crop coefficient (Eq. (3))

Crop	λ_E	E_d	E_w	RMSE mm d^{-1}	R^2
Sorghum	0.170	1.7	3.1	0.4	0.71
Oilseeds	0.362	0.6	4.5	0.4	0.95
Pulses	0.157	1.3	4.5	0.3	0.92
Crop	**λ_K**	**K_d[a]**	**K_w**	**RMSE**	**R^2**
Sorghum	0.916	0.55	0.49	0.12	0.49
Oilseeds	1.719	0.21	0.96	0.12	0.87
Pulses	0.867	0.41	0.81	0.08	0.87

[a] Potential evapotranspiration for calculating K_d and K_w was based on net radiation from the surface radiation budget (SRB).

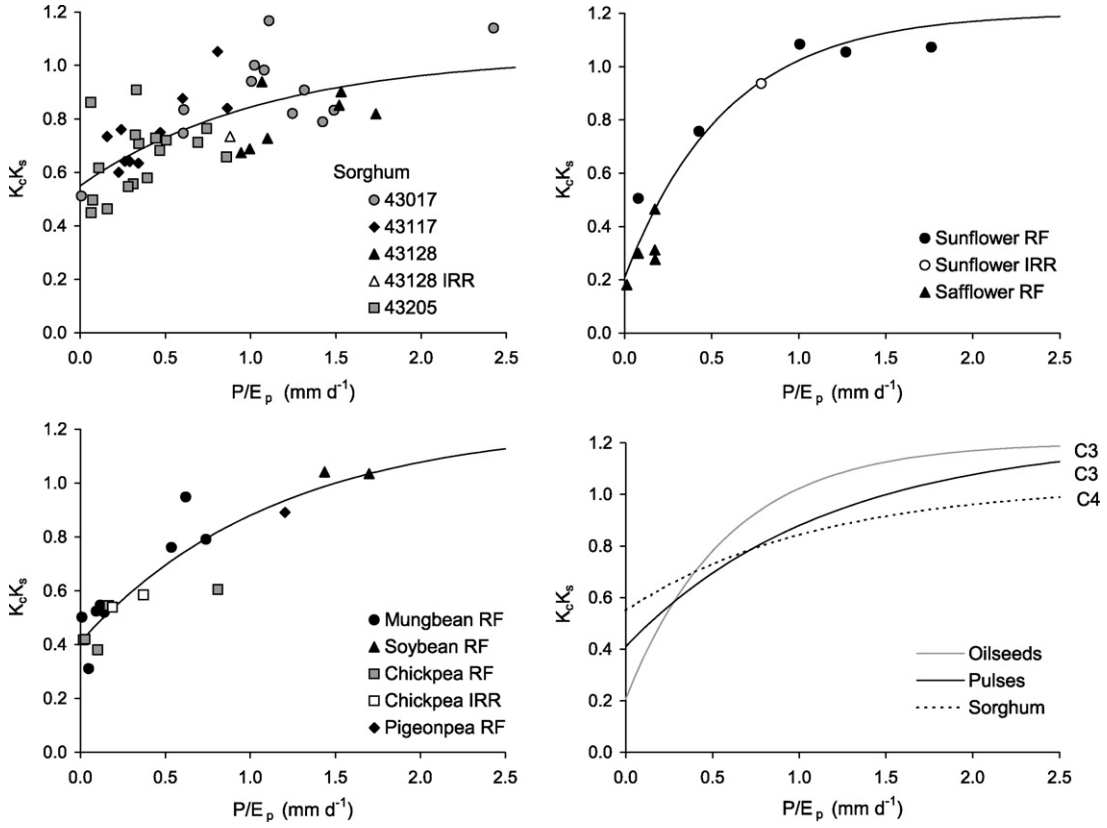

Fig. 4 – The ratio of seasonal precipitation to seasonal potential evapotranspiration (E_p) versus the combined crop coefficient (K_cK_s) observed in the lysimeter experiments. The lines indicate the model fits (Eq. (3)). Potential evapotranspiration was calculated using radiation estimated from satellite methods (SRB).

4.2. *Potential evapotranspiration and crop coefficients by radiation method*

Potential evapotranspiration (E_p) values differed by the method used to determine net radiation (R_n) (Table 2, Fig. 5). The mean monthly E_p calculated from the ground-based, empirical methods (E_pGBE) was 7–20% higher than E_p that used radiation from the satellite-based measurements (E_pSRB) depending on the month. The difference between E_p between the two methods was smallest during the monsoon season and largest at the end of the dry season. The difference in net radiation between the SRB and GBE methods was due to differences in their estimates of net longwave radiation, which was more negative for the SRB, particularly during the post-monsoon season.

Seasonal K_c values calculated using E_pGBE were only slightly (2–4%) lower than the K_c values calculated using E_pSRB because K_c was determined by evapotranspiration from crops grown during the monsoon, when the difference in E_p by the two radiation methods was smallest. The difference in E_p and the resulting modeled K_s would be larger during the post-monsoon. Thus, while a single K_c value could be used to

Table 4 – Seasonal crop coefficients (K_c) by method used to determine net radiation, and comparisons with literature values of K_c

	This study		Other studies in India	FAO-56 (Allen et al., 1998)	
	GBE[a]	SRB		Default	FAO_{adj}[b]
Sorghum	0.97	0.99	0.92[c]	0.97	0.95
Oilseeds	1.10	1.14	0.93[d]	0.86	0.76
Pulses	1.09	1.11	1.02[e]	0.81	0.70

[a] GBE and SRB indicate K_c values calculated from potential evapotranspiration using net radiation from ground-based empirical equations (GBE) or satellite methods (SRB), respectively.
[b] FAO_{adj} is the default K_c adjusted for relative humidity and temperature at the lysimeter stations in the Krishna Basin.
[c] Tyagi et al. (2000b).
[d] Tyagi et al. (2000a).
[e] Red gram, Singandhupe and Sethi (2005).

Please cite this article in press as: Biggs, T.W. et al., Evapotranspiration and regional probabilities of soil moisture stress in rainfed crops, southern India, Agric. Forest Meteorol. (2008), doi:10.1016/j.agrformet.2008.05.012

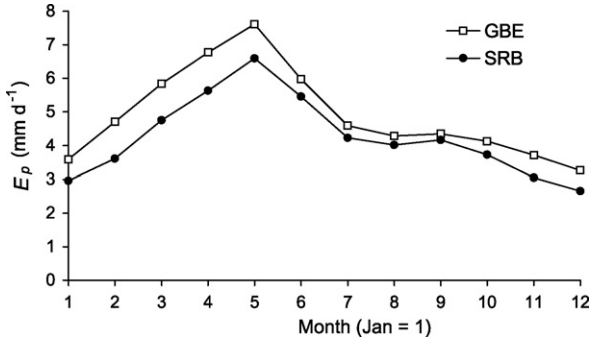

Fig. 5 – Average daily potential evapotranspiration (E_p) by month estimated by the Penman–Monteith equation and two different methods to estimate radiation: satellites (E_pSRB) and ground-based, empirical equations (E_pGBE). Values are the average of the E_p at the four lysimeter stations.

calculate E_a using either radiation method, the parameters of the $K_cK_s - E_p/P$ curves (Eq. (3)), particularly those that control the form of the curve under low seasonal precipitation, were specific to the radiation method used to calculate E_p.

4.3. *Probability distributions of P and K_s*

Precipitation during the *kharif* season (July–October) taken from the CRU grids (1901–2000) fit gamma probability distributions, while the soil moisture coefficient for sorghum (K_s) was left-skewed and fit a beta distribution (Fig. 6). The long left tail of the probability distribution of K_s was due to the asymptotic shape of the $K_cK_s - P/E_p$ curve (Fig. 4).

The cumulative probability distributions (cdf) of K_s for each 0.5° cell were used to generate maps of the probability of mild ($K_s < 0.8$) or moderate ($K_s < 0.6$) soil moisture stress during the

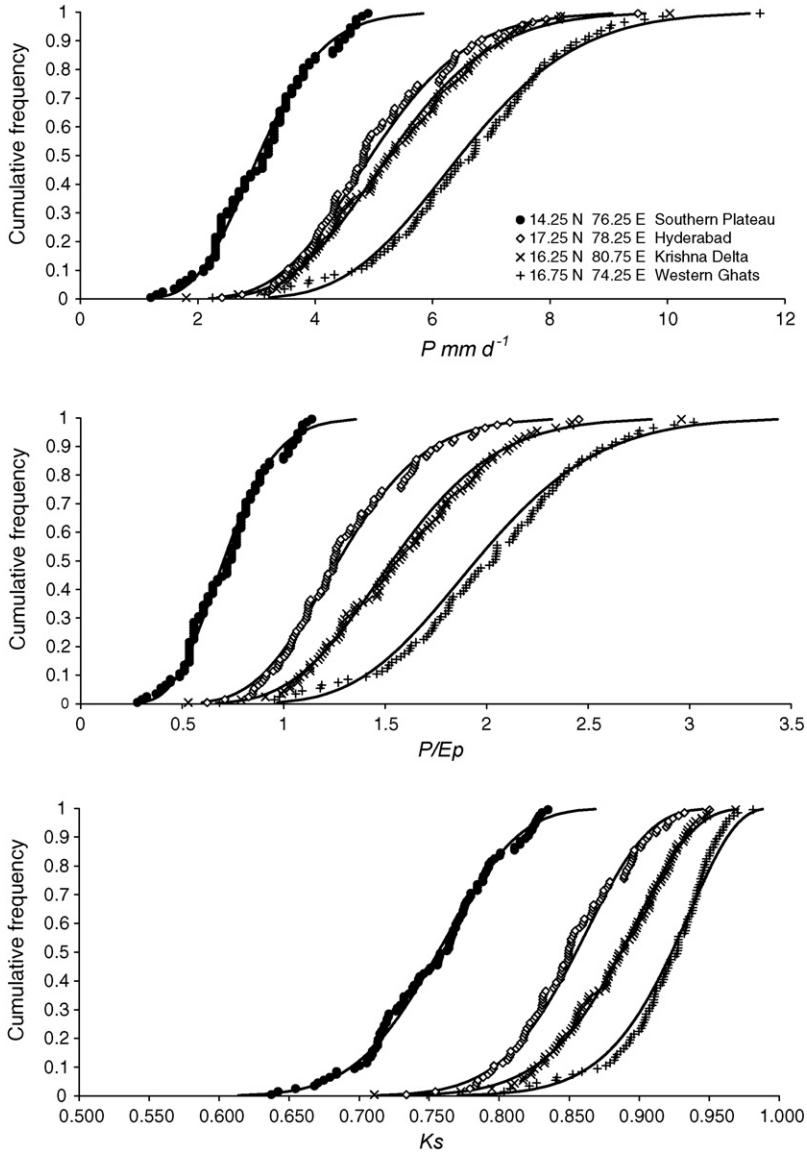

Fig. 6 – Cumulative distributions of seasonal precipitation (mm d^{-1}), the ratio of precipitation to potential evapotranspiration, and K_s for four different locations in the Krishna Basin, during the monsoon (*kharif*) season (July–October) over 1901–2000. The precipitation data was from the Climate Research Unit and was fit to a Gamma distribution. K_s was fit to a Beta distribution.

Please cite this article in press as: Biggs, T.W. et al., Evapotranspiration and regional probabilities of soil moisture stress in rainfed crops, southern India, Agric. Forest Meteorol. (2008), doi:10.1016/j.agrformet.2008.05.012

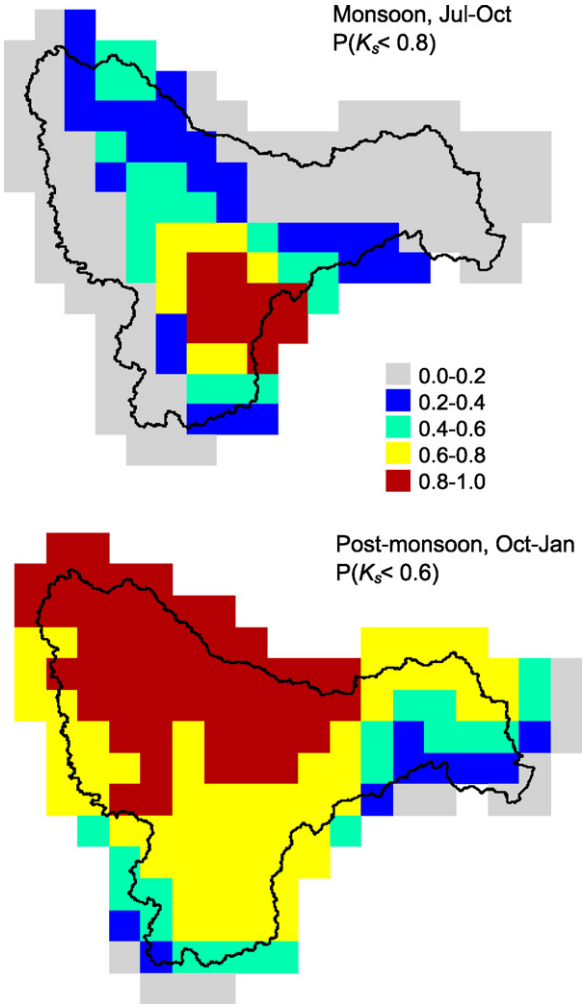

Fig. 7 – Maps of the probability of a sorghum crop experiencing (A) mild moisture stress (K_s < 0.80) during the monsoon (*kharif*) season, and (B) moderate moisture stress (K_s < 0.6) during the post-monsoon (*rabi*) season. Each grid cell is 0.5°.

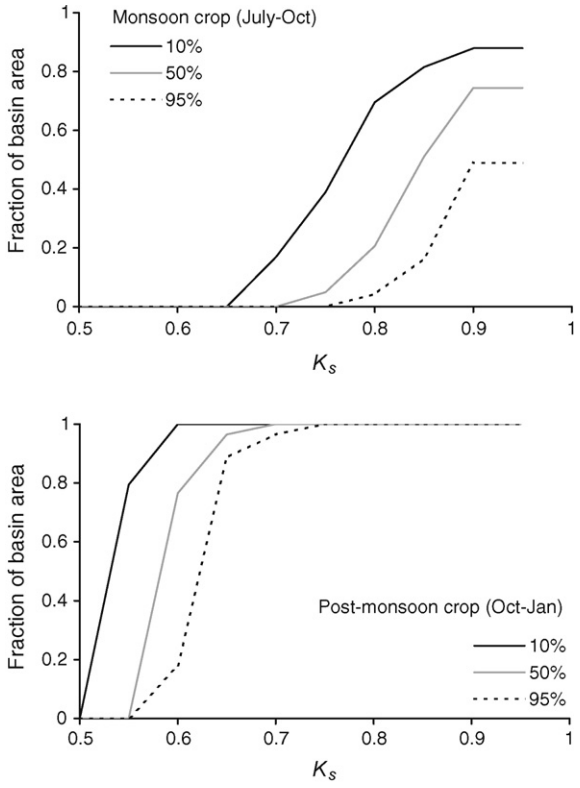

Fig. 8 – Fraction of the area of the Krishna Basin with a given soil moisture coefficient (K_s). Different lines indicate different probabilities of occurrence. For example, the black lines indicate the fraction of the basin that has a 10% chance of having a given K_s value in a given year.

monsoon and post-monsoon seasons, respectively (Fig. 7). The terms "mild stress" for K_s of 0.8 and "moderate stress" for K_s of 0.6 are qualitative, and do not quantitatively describe the impacts on yield. The relatively dry south-central plateau showed lower mean precipitation and higher probability of mild soil moisture stress during the monsoon season. During the post-monsoon (*rabi*) season, the central and northwestern parts of the basin showed the highest probability of moderate soil moisture stress.

The spatially distributed probability distributions suggested that 20% of the basin area had a 50% chance of experiencing at least mild soil moisture stress ($K_s < 0.8$) in a sorghum crop during any given *kharif* (monsoon) season, while a relatively small fraction of the basin (4%) had a 95% chance of experiencing mild moisture stress in any given *kharif* season (Fig. 8). A majority of the basin area (70%) had a 10% chance of experiencing mild moisture stress during the *kharif* season. This suggests that supplemental irrigation would alleviate mild or greater moisture stress in 1 year out of 10 over 70% of the basin area, in 1 year in 2 over 20% of the basin, and nearly every year over 4% of the basin. Note that this does not imply that mild moisture stress will occur in 70% of the basin in a single year, but rather that 70% of the basin area has a one in ten probability of mild moisture stress in any given year. The spatial distribution of moisture stress in a given year depends on the spatial autocorrelation structure of seasonal precipitation, so the spatial pattern in K_s in a given year would likely differ somewhat from the maps of long-term probabilities of K_s (Fig. 6). The maps of the probabilities of soil moisture stress apply to areas within each 0.5° cell where soil characteristics (texture, organic matter and depth) are similar to the soil used in the lysimeter experiments. The implications of this are discussed below.

4.4. *Limitations of the method and applicability to other regions*

The method used here has limitations similar to other empirical methods that use calibrated models to predict soil moisture stress. The limitations fall into four major categories: (1) spatial variability of model parameters, (2) variance in soil moisture stress not accounted for by the regression model, (3) the relationship between soil moisture stress and yield, and (4) the effect of climate change on the probability distributions of precipitation and moisture stress.

Please cite this article in press as: Biggs, T.W. et al., Evapotranspiration and regional probabilities of soil moisture stress in rainfed crops, southern India, Agric. Forest Meteorol. (2008), doi:10.1016/j.agrformet.2008.05.012

First, we assumed that the three model parameters (K_d, K_w, and λ_E) were constant over the basin. Soil texture, depth and the temporal distribution of rainfall within a month may differ among or within the 0.5° cells, which could change the model parameters and the resulting probability maps of K_s. The lysimeter measurements from the four stations were lumped to generate regional $K_cK_s - P/E_p$ relationships, though there is almost certainly spatial variability in the relationships not captured with the available data. Areas with shallow or sandy soils are particularly likely to have different model parameters and a higher probability of moisture stress than areas with soils similar to those used in the lysimeters. Some soils in the northwestern part of the basin are shallow (<0.5 m, Fig. 2) and crops grown there may be more prone to soil moisture stress for a given precipitation depth than the crops grown in the lysimeters. However, some proportion of each 0.5° cell in the basin contains moderately deep to deep soil, including valley bottoms in the northwest (Fig. 2), so the probability maps are likely valid for these areas in each cell. The model parameters for areas with shallow soils could be derived from either other lysimeter experiments in southern India, or from a more complex model that explicitly tracks soil moisture volumes. Ideally, the model parameters would be estimated for the soils that are actually cropped in sorghum, rather than for all soils in a 0.5° grid cell. Cropped area derived from satellite imagery could be incorporated to generate probabilities of moisture stress where sorghum is actively cropped.

Secondly, some of the variance in E_a and K_s was not captured by the regression models. The regional models predicted the mean K_s for a given depth of seasonal precipitation, though some K_s values observed in the lysimeter experiments were significantly lower than the mean (Fig. 4). Some of the unexplained variability in K_s may be due to the temporal distribution of daily rainfall within the month, especially the length of dry spells and mean depth of events, both of which influence soil moisture dynamics (Rodriguez-Iturbe et al., 2001). The unexplained variance may result in underestimation of the probability of moisture stress in some parts of the basin.

Thirdly, the average soil moisture stress over a season may not accurately estimate its impact on yield. Yield can be a complex function of the timing of precipitation (Vaux and Pruitt, 1983) or soil moisture stress (Garrity et al., 1982), though seasonal evapotranspiration often explains the majority of the variance in yield (Doorenbos and Kassam, 1979), and seasonal estimates of soil moisture may be sufficient to estimate yields (Oosterom et al., 1996). Data on crop yields for different K_s values could be modeled using data from the literature (e.g., Doorenbos and Kassam, 1979) or calculated from lysimeter experiments that included measurements of yield.

Finally, the probability distributions of precipitation and moisture stress are based on a dataset covering 1901–2000. Any shift in the probability distribution of precipitation due to natural fluctuations or anthropogenic greenhouse gas forcing (Mandke et al., 2007) could change the probability distributions of soil moisture stress. The regression model (Eq. (3)) could be used to assess the impact of any changes in precipitation on the long-term probability of moisture stress.

5. Conclusion

A central premise of this paper is that anticipation of the likelihood of moisture stress and planning for supplemental irrigation at the basin scale require a probabilistic perspective. Supplemental irrigation may not be required in all years, so its benefits are probabilistic and differ by location according to the climate. Understanding the spatial distribution of the probability of moisture stress is essential for planning supplemental irrigation at the basin scale. The modeling approach used here could complement regional snapshots of evapotranspiration, such as those provided by satellite imagery, which capture the spatial variability but not the full historical range of rainfall and soil moisture stress experienced over an area. Simple models of actual evapotranspiration based on seasonal precipitation and lysimeter data allowed us to leverage historical monthly precipitation datasets to generate long-term probability distributions of soil moisture stress over a large river basin. The simplicity of the modeling approach allowed application to areas where daily rainfall and detailed soil data were not available. Currently, forecasts of precipitation in India (Basu, 2005; Kumar et al., 2005; Rajeevan et al., 2004) and other regions (Nnaji, 2001) predict seasonal precipitation, so forecasts of soil moisture stress can also be made with simplified seasonal models of the kind presented here. The regional maps provide a basis for estimating probability distributions of the yields of rainfed crops, and for examining the potential benefits and hydrological consequences of irrigation in different parts of a river basin.

Acknowledgements

This research was performed in part during a post-doctoral fellowship of Biggs at the International Water Management Institute (IWMI) in Hyderabad, India, and support of colleagues at IWMI and the International Crops Research Institute for the Semi-Arid Tropics (ICRISAT) is gratefully acknowledged. Students from the Jawaharlal Nehru Technological University in Hyderabad digitized the soil maps. The work was supported by a grant from the Australian Council for International Agricultural Research. Thanks to Chris Scott, David Molden, and Frank Rijsberman of IWMI for support, and to Terressa Whitaker and two anonymous reviewers for helpful comments.

REFERENCES

Allen, R.G., Pereira, L.S., Raes, D., Smith, M., 1998. Crop Evapotranspiration. Irrigation and Drainage Paper 55. Food and Agriculture Organization, Rome.

Allen, R.G., Pruitt, W.O., Jensen, M.E., 1991. Environmental requirements of lysimeters. In: Allen, R.G., Howell, T.A., Pruitt, W.O., Walter, I.A., Jensen, M.E. (Eds.), ASCE Specialty Conference on "Lysimeters for Evapotranspiration and Environmental Measurements", Honolulu, Hawaii, pp. 170–181.

Please cite this article in press as: Biggs, T.W. et al., Evapotranspiration and regional probabilities of soil moisture stress in rainfed crops, southern India, Agric. Forest Meteorol. (2008), doi:10.1016/j.agrformet.2008.05.012

Bastiaanssen, W.G.M., Ahmad, M.D., Chemin, Y., 2002. Satellite surveillance of evaporative depletion across the Indus Basin. Water Resources Research 38 (12), 1273, doi:10.1029/2001WR000386.

Basu, B.K., 2005. Some characteristics of model-predicted precipitation during the summer monsoon over India. Journal of Applied Meteorology 44 (3), 324–339.

Biggs, T.W., Gaur, A., Scott, C.A., Thenkabail, P., Gangadhara Rao, R., Krishna Gumma, M., Acharya, S.K., Turral, H., 2007a. Closing of the Krishna Basin: irrigation development, streamflow depletion, and macroscale hydrology. In: IWMI Research Report 111, International Water Management Institute, Colombo, Sri Lanka.

Biggs, T.W., Scott, C.A., Rajagopalan, B., Turral, H., 2007b. Trends in solar radiation due to clouds and aerosols, Krishna River Basin, Southern India, 1952–1997. International Journal of Climatology 27 (11), 1505–1518.

Biggs, T.W., Thenkabail, P.S., Gumma, M.K., Scott, C., Parthasaradhi, G.R., Turral, H., 2006. Irrigated area mapping in heterogeneous landscapes with MODIS time series, ground truth and census data, Krishna Basin, India. International Journal of Remote Sensing 27 (10), 4245–4266.

Brugere, C., Lingard, J., 2003. Irrigation deficits and farmers' vulnerability in Southern India. Agricultural Systems 77 (1), 65–88.

Challa, O., Vadivelu, S., Sehgal, J., 1996. Soil Map of Maharashtra. National Bureau of Soil Survey (NBSS) and Land Use Planning Nagpur.

Dehghani Sanij, H., Yamamoto, T., Rasiah, V., 2004. Assessment of evapotranspiration estimation models for use in semi-arid environments. Agricultural Water Management 64 (2), 91–106.

Dewandel, B., Lachassagne, P., Wyns, R., Marechal, J.C., Krishnamurthy, N.S., 2006. A generalized 3-D geological and hydrogeological conceptual model of granite aquifers controlled by single or multiphase weathering. Journal of Hydrology 330 (1–2), 260–284.

Doorenbos, J., Kassam, A.H., 1979. Yield Response to Water. FAO, Rome.

Drexler, J.Z., Snyder, R.L., Spano, D., U., K.T.P., 2004. A review of models and micrometeorological methods used to estimate wetland evapotranspiration. Hydrological Processes 18 (11), 2071–2101.

Food and Agriculture Organization, 1995. Digital Soil Map of the World and Derived Soil Properties. Food and Agriculture Organization of the United Nations, Rome.

Fox, P., Rockström, J., 2003. Supplemental irrigation for dry-spell mitigation of rainfed agriculture in the Sahel. Agricultural Water Management 61 (1), 29–50.

Fox, P., Rockström, J., Barron, J., 2005. Risk analysis and economic viability of water harvesting for supplemental irrigation in semi-arid Burkina Faso and Kenya. Agricultural Systems 83 (3), 231–250.

Franks, S.W., Beven, K.J., Quinn, P.F., Wright, I.R., 1997. On the sensitivity of the soil-vegetation-atmosphere transfer (SVAT) schemes: equifinality and the problem of robust calibration. Agricultural and Forest Meteorology 86, 63–75.

Fu, Q., Liou, K.N., Cribb, M.C., Charlock, T.P., Grossman, A., 1997. Multiple scattering parameterization in thermal infrared radiative transfer. Journal of the Atmospheric Sciences 54 (24), 2799–2812.

Garatuza-Payan, J., Watts, C., 2005. The use of remote sensing for estimating ET of irrigated wheat and cotton in Northwest Mexico. Irrigation and Drainage Systems 19 (3–4), 301–320.

Garrity, D.P., Watts, D.G., Sullivan, C.Y., Gilley, J.R., 1982. Moisture deficits and grain sorghum performance: evapotranspiration-yield relationships. Agronomy Journal 74, 815–820.

Government of India, 1999. Soil Map of Andhra Pradesh. National Bureau of Soil Survey and Land Use Planning (ICAR), Bangalore.

Gupta, S.K., Ritchey, N.A., Wilber, A.C., Whitlock, C.H., Gibson, G.G., Stackhouse, P.W.J., 1999. A climatology of surface radiation budget derived from satellite data. Journal of Climate 12 (8), 2691–2710.

Hattendorf, M.J., Redelfs, M.S., Amos, B., Stone, L.R., Gwin Jr., R.E., 1988. Comparative water use characteristics of six row crops. Agronomy Journal 80 (1), 80–85.

Inman-Bamber, N.G., McGlinchey, M.G., 2003. Crop coefficients and water-use estimates for sugarcane based on long-term Bowen ratio energy balance measurements. Field Crops Research 83 (2), 125.

Kumar, K.K., Hoerling, M., Rajagopalan, B., 2005. Advancing dynamical prediction of Indian monsoon rainfall. Geophysical Research Letters 32 , doi:10.1029/2004GL021979.

Laio, F., Porporato, A., Ridolfi, L., Rodriguez-Iturbe, I., 2001. Plants in water-controlled ecosystems: active role in hydrologic processes and response to water stress, II, probabilistic soil moisture dynamics. Advances in Water Resources 24 (7), 707–724.

Loukas, A., Vasiliades, L., Domenikiotis, C., Dalezios, N.R., 2005. Basin-wide actual evapotranspiration estimation using NOAA/AVHRR satellite data. Physics and Chemistry of the Earth, Part B: Hydrology, Oceans and Atmosphere 30, 69–79.

Mandke, S.K., Sahai, A.K., Shinde, M.A., Joseph, S., Chattopadhyay, R., 2007. Simulated changes in active/break spells during the Indian summer monsoon due to enhanced CO_2 concentrations: assessment from selected coupled atmosphere-ocean global climate models. International Journal of Climatology 27 (7), 837–859.

Mitchell, T., Carter, T., Jones, P., Hulme, M., New, M., 2004. A comprehensive set of high-resolution grids of monthly climate for Europe and the globe: the observed record (1901–2000) and 16 scenarios (2001–2100), Working Paper 55, Tyndall Centre, University of East Anglia, Norwich, UK.

Mitchell, T.D., Jones, P.D., 2005. An improved method of constructing a database of monthly climate observations and associated high-resolution grids. International Journal of Climatology 25 (6), 693–712.

Mohan, S., Arumugam, N., 1994. Crop coefficients of major crops in South India. Agricultural Water Management 26 (1–2), 67–80.

New, M., Hulme, M., Jones, P., 1999. Representing twentieth-century space-time climate variability. Part I: development of a 1961–90 mean monthly terrestrial climatology. Journal of Climate 12 (3), 829–856.

New, M., Hulme, M., Jones, P.D., 2000. Representing twentieth century space-time climate variability. Part 2: development of 1901–96 monthly grids of terrestrial surface climate. Journal of Climate 13, 2217–2238.

Nnaji, A.O., 2001. Forecasting seasonal rainfall for agricultural decision-making in northern Nigeria. Agricultural and Forest Meteorology 107 (3), 193–205.

Oosterom, E.J., Bidinger, F.R., Mahalakshmi, V., Rao, K.P., 1996. Effect of water availability pattern on yield of pearl millet in semi-arid tropical environments. Euphytica 89 (2), 165–173.

Oweis, T., Pala, M., Ryan, J., 1998. Stabilizing rainfed wheat yields with supplemental irrigation and nitrogen in a Mediterranean climate. Agronomy Journal 90, 672–681.

Paco, T.A., Ferreira, M.I., Conceicao, N., 2006. Peach orchard evapotranspiration in a sandy soil: comparison between eddy covariance measurements and estimates by the FAO 56 approach. Agricultural Water Management 85 (3), 305–313.

Pereira, L.S., Oweis, T., Zairi, A., 2002. Irrigation management under water scarcity. Agricultural Water Management 57 (3), 175–206.

Please cite this article in press as: Biggs, T.W. et al., Evapotranspiration and regional probabilities of soil moisture stress in rainfed crops, southern India, Agric. Forest Meteorol. (2008), doi:10.1016/j.agrformet.2008.05.012

Rachidi, F., Kirkham, M.B., Stone, L.R., Kanemasu, E.T., 1993. Soil water depletion by sunflower and sorghum under rainfed conditions. Agricultural Water Management 24 (1), 49–62.

Rajeevan, M., Pai, D.S., Dikshit, S.K., Kelkar, R.R., 2004. IMD's new operational models for long-range forecast of southwest monsoon rainfall over India and their verification for 2003. Current Science 86 (3), 422–431.

Rodriguez-Iturbe, I., Porporato, A., Laio, F., Ridolfi, L., 2001. Plants in water-controlled ecosystems: active role in hydrologic processes and response to water stress. Advances in Water Resources 24 (7), 695–705.

Schulz, K., Beven, K., 2003. Data-supported robust parameterisations in land surface-atmosphere flux predictions: towards a top-down approach. Hydrological Processes 17 (11), 2259–2277.

Sehgal, J.L., Hirekerur, L.R., Sarma, V.A.K., 1996. Soil Map of Karnataka. National Bureau of Soil Survey, Nagpur.

Singandhupe, R.B., Sethi, R.R., 2005. Estimation of reference evapotranspiration and crop coefficient in wheat under semi-arid environment in India. Archives of Agronomy and Soil Science 51 (6), 619–631.

Singh, P., Alagarswamy, G., Pathak, P., Wani, S.P., Hoogenboom, G., Virmani, S.M., 1999. Soybean-chickpea rotation on Vertic Inceptisols: I. Effect of soil depth and landform on light interception, water balance and crop yields. Field Crops Research 63 (3), 211–224.

Stackhouse Jr., P.W., Gupta, S.K., Cox, S.J., Chiacchio, M., Mikovitz, J.C., 2001. The WCRP/GEWEX surface radiation budget project release 2: an assessment of surface fluxes at 1° resolution. National Aeronautics and Space Administration, Washington, DC.

Stewart, J.B., Watts, C.J., Rodriguez, J.C., De Bruin, H.A.R., van den Berg, A.R., Garatuza-Payan, J., 1999. Use of satellite data to estimate radiation and evaporation for northwest Mexico. Agricultural Water Management 38 (3), 181–193.

Supit, I., van Kappel, R.R., 1998. A simple method to estimate global radiation. Solar Energy 63, 147–160.

Tyagi, N., Sharma, D., Luthra, S., 2003. Determination of evapotranspiration for maize and berseem clover. Irrigation Science 21 (4), 173–181.

Tyagi, N.K., Sharma, D.K., Luthra, S.K., 2000a. Determination of evapotranspiration and crop coefficients of rice and sunflower with lysimeter. Agricultural Water Management 45 (1), 41–54.

Tyagi, N.K., Sharma, D.K., Luthra, S.K., 2000b. Evapotranspiration and crop coefficients for wheat and sorghum. Journal of Irrigation & Drainage Engineering 4, 215–222.

Vaux, H.J., Pruitt, W.O., 1983. Crop-water production functions. Advances in Irrigation 2, 61–97.

Wood, S., Sebastian, K., Scherr, S.J., 2000. Pilot Analysis of Global Ecosystems: Agroecosystems. World Resources Institute and International Food Policy Research Institute, Washington, DC.

Zhang, J., Kirkham, M.B., 1995. Water relations of water-stressed, split-root C4 (Sorghum bicolor; Poaceae) and C3 (Helianthus annuus; Asteraceae) plants. American Journal of Botany 82 (10), 1220–1229.

Please cite this article in press as: Biggs, T.W. et al., Evapotranspiration and regional probabilities of soil moisture stress in rainfed crops, southern India, Agric. Forest Meteorol. (2008), doi:10.1016/j.agrformet.2008.05.012